



Mechanical and optical properties of a borosilicate glass used to improve the finishing of 3Y-TZP restorations

Ana Carolina da SILVA^(a) 
Camila da Silva RODRIGUES^(a) 
Juliana de Freitas Gouveia SILVA^(a) 
Clarice Ferreira SABINO^(a) 
Gilmar Patrocínio THIM^(b) 
Renata Marques de Melo MARINHO^(a) 
Tiago Moreira Bastos CAMPOS^(b) 

^(a)Universidade Estadual Paulista – Unesp,
Institute of Science and Technology,
Department of Dental Materials and
Prosthodontics, São José dos Campos,
SP, Brazil.

^(b)Instituto Tecnológico de Aeronáutica – ITA,
Physics Department, São José dos Campos,
SP, Brazil.

Declaration of Interests: The authors certify that they have no commercial or associative interest that represents a conflict of interest in connection with the manuscript.

Corresponding Author:

Renata Marques de Melo
E-mail: renata.marinho@ict.unesp.br

<https://doi.org/10.1590/1807-3107bor-2024.vol38.0077>

Abstract: Borosilicate glass was developed to enhance the mechanical behavior and smoothness of dental zirconia as an alternative to conventional glaze. This study assessed the mechanical and optical properties of 3 mol% yttria-stabilized tetragonal zirconia polycrystal (3Y-TZP) coated with borosilicate glass or a commercial glaze fired for an extended period of time. Disc-shaped 3Y-TZP zirconia specimens (Zpex, Tosoh) were sintered at 1550°C for 2 hours. The specimens were divided into three groups: as-sintered (control, C); commercial glaze (G); and borosilicate glass (SL). The glaze and borosilicate glass were applied over the zirconia and fired for 20 minutes at 950°C and 1200°C, respectively. Biaxial flexural strength, fractography, X-ray diffraction (XRD), roughness (Ra and Rz), fracture toughness (Vickers indentation method), color difference (ΔE_{00}), and translucency (TP_{00}) analyses were conducted. The t-test or the one-way ANOVA and Tukey's tests were used to analyze the data ($\alpha = 0.05$). Flexural strength data were subjected to the Weibull analysis. The SL group exhibited the highest flexural strength (1025.8 MPa), whereas the C (859.41 MPa) and G (816.0 MPa) groups exhibited similar values. The SL group also had the highest characteristic strength. The fracture origin in all groups was on the zirconia surface. XRD analysis revealed that the specimens from the SL group contained tetragonal, cubic, and monoclinic phases. The SL group presented the lowest surface roughness. Fracture toughness in the SL group was lower than in the C group, but similar to that observed in the G group. The translucency and color differences observed in the G and SL groups were similar. Borosilicate glass enhanced the flexural strength of 3Y-TZP, promoted the smoothest surface, and exhibited optical properties similar to those of the glaze.

Keywords: Boron; Glass; Mechanical Test; Ceramics.

Introduction

The biomimetic and mechanical properties of dental materials significantly impact the success of oral rehabilitations. Dental zirconia, commonly employed as a restorative material, particularly in monolithic restorations, often necessitates additional laboratory finishing procedures such as stains, glaze application, or polishing with rubber points to achieve a natural appearance. Beyond their aesthetic significance, these techniques

Submitted: July 11, 2023
Accepted for publication: November 11, 2023
Last revision: February 12, 2024



may also influence the clinical and mechanical behavior of dental ceramics.¹⁻³

Glazing enhances the clinical outcome of dental ceramic restorations by smoothing the surface, resulting in a glossy and natural final appearance.⁴ Previous studies have indicated that glazing does not impact the fatigue behavior of 3% mol yttrium-stabilized tetragonal zirconia polycrystals (3Y-TZP).^{2,5} However, concerns regarding opposing tooth wear and internal flaws have been raised in relation to the glaze layer.⁶⁻⁸ The weak interaction between zirconia and glaze creates a region of fragility, potentially leading to delamination or the formation of critical defects.⁸

Extended glaze firings have been proposed as an alternative method for finishing ceramic restorations.⁹⁻¹¹ Studies have shown that extended glaze firing can enhance flexural strength and reduce tensile residual stresses at the surface of porcelain-veneered zirconia.¹¹ This technique involves adjusting the glaze firing process by prolonging the holding time at the maximum temperature, typically from 1 to approximately 15 minutes.⁹⁻¹¹ According to Callister and Rethwisch,¹² when glasses are heated to a temperature close to that of their softening point, stresses are alleviated within approximately 15 minutes, known as the “annealing point”.

In an effort to enhance the mechanical properties of dental zirconia without compromising its optical characteristics, novel compositions of glass materials for finishing have been developed.^{8,13} During the development of these glasses, various ion concentrations can be incorporated into their compositions to achieve specific final characteristics. This is possible because the glass structure does not depend on a particular stoichiometry.¹⁴ Glasses that are boron-doped are commonly referred to as Pyrex.¹⁵ When utilized as a dopant in a glass matrix, boron (B) has the ability to alter the intrinsic properties of the material. Consequently, borosilicate glass forms a stable material at elevated temperatures with a low coefficient of thermal expansion (CTE; $3.25 \times 10^{-6} \text{ K}^{-1}$).^{15,16}

The application of a low-CTE glass, such as borosilicate glass, onto zirconia (CTE: $10.8 \times 10^{-6} \text{ K}^{-1}$) tends to enhance the mechanical performance of the

set.¹⁷ Borosilicate glass application on ceramics is a well-established method for inducing compression stress at the surface, thereby favoring the mechanical properties of the material.¹⁸ The borosilicate glass used in this study represents an advancement over the experimental glaze developed by Campos et al.⁸ In previous studies, the thermally compatible glaze was calcinated at 1530°C, whereas the borosilicate glass was fired at 1,200°C, a temperature close to the glaze and stain characterization range (850–950°C).^{8,13} The biaxial flexural strength provided by the borosilicate layer exhibited values 14% higher than that of the experimental glaze calcinated at 1530°C. In contrast, conventional glazing of zirconia does not contribute to an increase in the mechanical strength of the materials.^{2,5}

Nevertheless, the application method for the developed borosilicate glass described herein is similar to the glaze slurry method, yet it has the capability to generate an even smoother surface and enhance the mechanical strength of zirconia. This innovation represents a more user-friendly application technique, making it easier for dental technicians.

Hence, a borosilicate glass was developed for application as an alternative finishing material for 3Y-TZP zirconia, aiming to enhance mechanical properties in comparison to both glaze and no coating. Accordingly, the aim of this study was to assess the mechanical and optical properties of 3Y-TZP coated with an experimental borosilicate glass and a commercial glaze subjected to an extended firing time. As-sintered specimens served as controls. Complementary analyses, encompassing optical properties, roughness, crystalline content, and fracture toughness, were conducted. The tested hypothesis posited that the zirconia specimens coated with borosilicate glass would have better mechanical properties and reduced roughness compared with those from the other study groups, without altering their optical properties.

Methodology

This *in vitro* study assessed the impact of surface treatment factors (experimental borosilicate glass, commercial glaze, or as-sintered) on various

Table 1. Description of the materials used in the study.

Materials	Composition	Manufacturer	Batch number
Zirconia 3Y-TZP	90.4–94.5 wt% ZrO ₂ ; 4–6 wt% Y ₂ O ₃ ; 1.5–2.5 wt% HfO ₂ ; 0–0.3 wt% Al ₂ O ₃ ; 0 wt% Er ₂ O ₃ ; 0–0.3 wt% Fe ₂ O ₃	Zpex (ZPex, Tosoh Corporation, Tokyo, Japan)	ZY308567B
Glassy-based material applied by brush	Special low fusing glaze material to create a silky matte and sealed surface	Vita Akzent (Akz 25), VITA Zahnfabrik, Bad Sackingen, Germany	38030 powder 22601 building liquid
Borosilicate glass	SiO ₂ -68%; Al ₂ O ₃ -1.1%; CaO 8.93%; Na ₂ O -14.54%, MgO -3.41%, K ₂ O -0.59% and B ₂ O ₃ -4%.	Developed by authors	-
Propylene glycol solution	C ₃ H ₈ O ₂	Labsynth, Diadema, São Paulo, Brazil	178730

outcomes, including flexural strength, roughness, translucency, color change, and toughness. Table 1 provides details on the materials utilized in this study, including their composition, manufacturers, and batch numbers.

Preparing the borosilicate glass powder

The borosilicate glass was obtained using a silicic acid source, following the methodology developed by Campos et al.¹⁹ The corresponding salts were incorporated, and the final composition of the borosilicate glass comprised SiO₂ (68%), Al₂O₃ (1.1%), K₂O (0.59%), Na₂O (14.54%), CaO (8.93%), MgO (3.41%), and B₂O₃ (4%). The glass underwent a heat treatment in an oven at 100°C for 24 hours, followed by calcination at 600°C for 5 hours. Subsequent to this process, the material was ground in an alumina mortar and sieved through a 200-mesh screen.

Zirconia disc preparation

A total of 0.85 g of 3Y-TZP zirconia powder (ZPex, Tosoh Corporation, Tokyo, Japan) underwent uniaxial pressing for 30 s at 1148 kgf. A tungsten carbide cylindrical matrix measuring 9 cm in height and 5 cm in diameter and having a retractable base, an internal piston, and an internal hole for disc pressing was used to produce discs measuring 15 mm in diameter by 1.5 mm in thickness (n = 90). The discs were subsequently sintered at 1550°C for 2 hours (Sirona inFire HTC speed), and were then randomly distributed into three groups (n = 30) based on the subsequent surface treatment applied to them: commercial glaze with extended firing (G group), experimental borosilicate glass (SL group), or as-sintered, representing the control specimens

(C group). The final dimensions of the specimens were 12 mm in diameter by 1.2 mm in thickness (ISO 6872).

Glaze and borosilicate glass application

For the G group, 0.18 g of glaze powder (Vita Akzent GLAZE, VITA Zahnfabrik, Bad Sackingen, Germany) was mixed with 5 drops of building liquid (Vita Akzent FLUID, VITA Zahnfabrik, Bad Sackingen, Germany) until achieving a homogeneous consistency. Subsequently, a thin layer of the mixture was applied to one surface of the zirconia discs using a fine-tipped brush. The discs underwent firing in a vacuum furnace using the following settings: 400°C initial temperature, 5-minute heating time, 80°C/min temperature elevation rate, 950°C final temperature, and a 20-minute dwell time at the final temperature.

For the SL group, 0.20 g of borosilicate glass powder was mixed with 0.20 g of propylene glycol (P.A.-A.C.-S, Labsynth, Diadema, Brazil). This mixture was then applied with a brush following the same procedure as that described for the glaze groups. The discs underwent firing with the following settings: 400°C initial temperature, 5-minute heating time, 80°C/min temperature elevation rate, 1200°C final temperature, and a 20-minute dwell time at the final temperature. A pilot study was conducted to determine a final temperature that would yield a smooth and aesthetically pleasing appearance.

A previously trained operator performed the glaze and experimental glass applications. The final thickness of the specimens was measured using a digital caliper [G: 1.39 (0.05) mm, SL: 1.37 (0.05) mm]. The appearance of the specimens from each group is depicted in Figure 1.

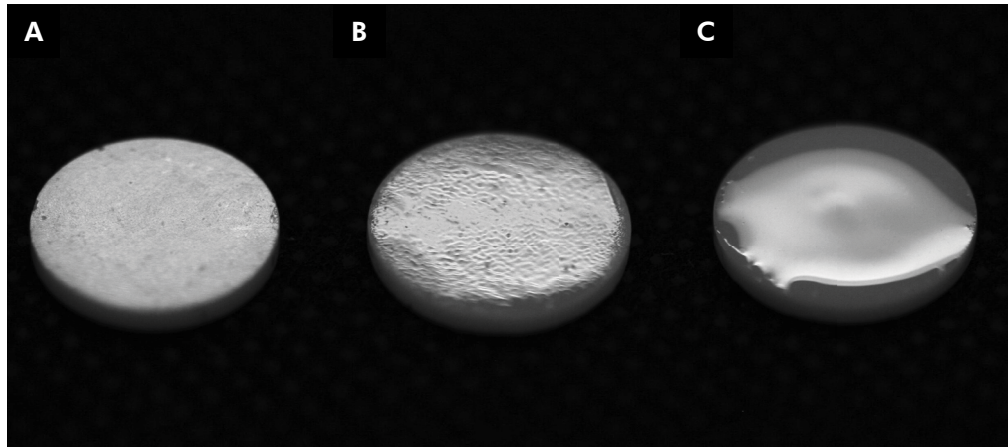


Figure 1. Final appearance of the 3Y-TZP specimens: as-sintered (a), coated with glaze (b), and coated with borosilicate glass (c).

Roughness analysis

All the specimens from each group ($n = 30$) were analyzed using a contact roughness tester (SJ 400, Mitutoyo, Tokyo, Japan). Three equidistant parallel measurements were taken for each specimen at a speed of 0.2 mm/s, and an additional three parallel measurements were taken with the same specimen rotated by 90 degrees. The analysis adhered to ISO 4287-1997 standards, employing a Gaussian filter and a cut-off wavelength value of 0.8 mm. Average values were computed for each sample, and the mean Ra (average roughness) and Rz (ten-point-mean roughness) values were utilized in the subsequent statistical analysis.

X-ray diffraction analysis (XRD)

Two specimens from each group were analyzed using X-ray diffractometry to identify the crystalline phases. Cu $K\alpha$ radiation with a wavelength of 0.15418 nm was employed within a range (-2) spanning 20° to 40° . The scanning parameters were a step of 10.1600 s, a step size of 0.0170° , scanning speed of 2°min^{-1} , 40 kV, and 40 mA.

The XRD data underwent analysis by identifying the crystalline phases after comparing the experimental spectra with standard diffraction spectra from the JCPDS (Joint Committee on Powder Diffraction Standards) and ICSD (Inorganic Crystal Structure). The High Score software program (Philips X'pert PANalytical, Almelo, The Netherlands) was utilized to obtain the spectral attributions.

Color and translucency measurement

The samples ($n = 30$) were assessed using a spectrophotometer (VITA Easyshade, Vita Zahnfabrik, Bad Säckingen, Germany). CIE $L^*a^*b^*$ coordinates (International Commission on Illumination) were recorded, where L^* represents the luminosity axis with values ranging from 0 (black) to 100 (white), and a^* and b^* denote the color coordinates along the green-red and blue-yellow axes, respectively. Measurements were taken over black ($L^* = 27.94$, $a^* = -0.01$, $b^* = 0.03$), white ($L^* = 92.95$, $a^* = 0.78$, $b^* = 3.57$), and gray ($L^* = 50.30$, $a^* = -1.41$, $b^* = -2.37$) backgrounds. The observer angle was set at 10° , and the chosen illuminant was D65. A coupling solution (glycerol, $\text{C}_3\text{H}_8\text{O}_3$, Vetec Química Fina Ltda, Rio de Janeiro, Brazil) was used between the specimen and the background to minimize light scattering.

Each specimen underwent three measurements, and the average $L^*a^*b^*$ values were utilized in the translucency and color difference calculations. The color differences (ΔE_{00}) between the control and experimental groups were computed using CIEDE 2000 (Eq. 1) based on measurements taken over a gray background. For clinical interpretation, the perceptibility ($\Delta E_{00} > 0.8$) and unacceptability ($\Delta E_{00} > 1.8$) thresholds established by Paravina et al. (2019) were taken into consideration.²⁰

$$\Delta E_{00} = \left[\left(\frac{\Delta C'}{K_L S_L} \right)^2 + \left(\frac{\Delta H'}{K_H S_H} \right)^2 + R_T \left(\frac{\Delta C'}{K_C S_C} \right) \left(\frac{\Delta H'}{K_H S_H} \right) \right]^{1/2} \text{ Eq. (1)}$$

where $\Delta L'$, $\Delta C'$ and $\Delta H'$ are the differences in luminosity, chroma, and hue, respectively, for a pair of measurements; RT is a rotation function accounting for the interaction between chroma and hue differences in the blue region; SL, SC, and SH are weighting functions adjusting the total color difference for variations in the location of the color difference pair in L^* , a^* , b^* coordinates; and k_L , k_C , and k_H are the parametric factors serving as correction terms for deviation from reference experimental conditions.

Measurements conducted over black and white backgrounds were employed to calculate the translucency parameter (TP_{00}) for each experimental group using CIEDE 2000 (Eq. 1). The simple translucency difference (ΔTP_{00}) between the experimental groups (SL or G) and the control group was computed for clinical interpretation, where $\Delta TP_{00} > 0.62$ was considered the perceptibility threshold, and $\Delta TP_{00} > 2.62$ was considered the unacceptability threshold.²¹

Biaxial flexural strength

The biaxial flexural strength test ($n = 30$) was conducted using a piston-on-three-ball setup (ISO 6872/2015). The samples were positioned with the coated surface on a circular base featuring three equidistant metallic spheres ($\mathcal{A}E = 3.2$ mm), forming a plane. The load was applied with a flat-tip piston ($\mathcal{A}E = 1.6$ mm) fixed on a universal testing machine (EMIC DL-1000, EMIC, Sao Jose dos Pinhais, Brazil) equipped with a load cell (1.000 kgf). The load was applied at a constant speed of 1 mm/min until fracture. All the tests were conducted under water. The biaxial flexural strength (σ , MPa) of the discs was determined using Eq. (2).

$$\sigma = -0.2387 P \left(X - \frac{Y}{d^2} \right) \quad \text{Eq. (2)}$$

where P is the load (N), X and Y are the parameters related to the elastic properties of the material [Poisson's ratio (0.3) and elastic modulus (210 GPa)], and d is the thickness of the specimen at the fracture origin (mm).

The fractured specimens were inspected using a stereomicroscope (Discovery V20, Carl Zeiss, Jena, Thuringia, Germany), and representative specimens ($n = 1$) were further evaluated in a scanning electron

microscope (SEM) to determine the failure origin and characteristics (fractography).

Fracture toughness

An additional set of specimens ($n = 10$) was prepared to assess fracture toughness. Five Vickers indentations were made with varying loads (C group, 9.8 N for 15 s; G group, 4.9 N for 15 s; SL group, 0.0987 N for 15 s) using an HMV-G21 instrument (Shimadzu, Kyoto, Japan). The length of the developed cracks was measured, and fracture toughness was estimated using Eq. (3), with the respective control values incorporated into the calculations.

$$K_{Ic} = k \left(\frac{E}{H} \right)^{0.5} \times \frac{P}{c^{3/2}} \quad \text{Eq. (3)}$$

where E is the elastic modulus, P is the applied load (in N), H is the Vickers hardness, given by $H = 1.8544P/a^2$ (in GPa), c is the average radial crack length measured from the center of the indentation (in m), and k is a constant equal to 0.016. The E values used for each group were $C = 200$ GPa,²² $G = 60$ GPa,²³ and $SL = 51$ GPa.²⁴

Statistical analysis

The statistical analysis was conducted using SigmaPlot 12.0 software (Systat Software Inc., San Jose, USA), and a significance level of 5%. Prior to analysis, the data were assessed for normality using the Shapiro-Wilk test, and for homoscedasticity using the Levene test. One-way ANOVA was employed to analyze flexural strength, translucency, roughness, and fracture toughness. A multiple comparison analysis was performed using Tukey's tests. Color difference data were analyzed using the t-test. Additionally, a Weibull analysis was applied to the flexural strength data, where Weibull's modulus and characteristic strength were obtained through a maximum likelihood estimation using Minitab 16 software (Minitab Inc., State College, USA), and a 95% confidence interval.

Results

The roughness results (R_a and R_z) are presented in Table 2. Borosilicate glass specimens had significantly

Table 2. Average roughness (Ra), ten-point-mean roughness (Rz), fracture toughness (K_{Ic}), biaxial flexural strength (BFS), Weibull modulus (m), and characteristic strength (σ_0) means, standard deviations, and confidence intervals (CI) obtained for the study groups. Different letters within a column indicate statistically significant differences among the study groups ($p < 0.05$, one-way ANOVA and Tukey's test).

Groups	Ra (μm)	Rz (μm)	K_{Ic} (MPa $\text{m}^{0.5}$)	BFS (MPa)	m CI (95%)	σ_0 CI (95%)
C	0.30 ^A (0.03)	2.13 ^A (0.20)	5.50 ^A (0.44)	859.41 ^A (157.57)	6.3 ^A (5.0–8.1)	920.8 ^A (865.7–979.3)
G	0.08 ^B (0.07)	0.43 ^B (0.31)	1.31 ^B (0.27)	816.0 ^A (97.22)	10.1 ^{AB} (8.1–12.6)	855.4 ^A (822.7–889.4)
SL	0.03 ^C (0.01)	0.18 ^C (0.10)	1.51 ^B (0.15)	1,025.8 ^B (122.85)	10.8 ^{AB} (8.6–13.4)	1072.2 ^B (1,033.1–1,113)

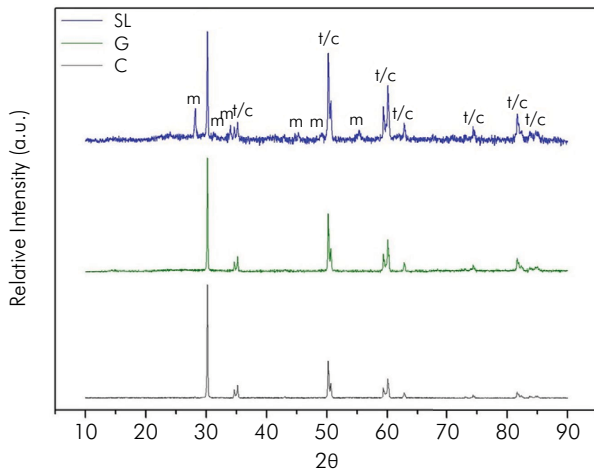


Figure 2. X-ray diffractograms from the study groups. The peaks represent tetragonal zirconia (t), cubic zirconia (c), and monoclinic zirconia (m).

lower values of Ra and Rz compared to specimens from the glaze and as-sintered groups ($p < 0.001$). The XRD analysis (Figure 2) demonstrated peaks characteristic of tetragonal zirconia in all groups. The presence of the cubic and monoclinic phases was observed exclusively in the SL group.

Table 3 outlines the translucency and color difference results obtained for the study groups. The translucency measurements for the control group were higher than those of the experimental groups ($p < 0.001$), which were similar to each other. However, the translucency differences of G and SL compared to C were not clinically perceptible. The color difference produced by glaze and borosilicate glass was statistically similar ($p = 0.116$) and clinically perceptible.

The flexural strength results are shown in Table 2. The as-sintered and glaze groups had similar strength

values ($p > 0.005$). The application of borosilicate led to the highest biaxial flexural strength values ($p < 0.001$). The characteristic strength of SL (1087) was significantly different compared to that of C (835.2) and G (852.3). However, the Weibull modulus of G (10.1) and SL (10.8) were similar (Table 2). Figure 3 illustrates the failure probability plot, highlighting the superior behavior of the SL group compared to the C group.

Figure 4 depicts the fractographic analysis. The fracture origin for all groups was identified on the zirconia, as highlighted by the yellow asterisk. A backscattered micrograph is displayed in Figure 4, e and f. Zirconia appears denser and is represented by a lighter color, whereas glaze can be identified by darker colors. The cross-section view revealed porosities in the glaze layer (Figure 4, e and f), whereas the borosilicate glass exhibited a more homogeneous glass layer (Figure 4, h and i).

Statistical differences in fracture toughness were observed among all groups ($p < 0.001$, Table 2). The values from the control group (as-sintered) were the highest, and were significantly different from those from both the glaze (G) and borosilicate glass (SL) groups.

Discussion

This study assessed the mechanical and optical characteristics of alternative surface finishings for dental zirconia. Borosilicate glass provided specimens with the highest flexural strength and smoothest surface, but did not contribute to an increase in fracture toughness. Additionally, its optical behavior was similar to that of the commercial glaze. Consequently, the tested hypothesis was partially accepted.

Table 3. Color difference (ΔE_{00}), translucency (TP_{00}), and translucency difference (ΔTP_{00}) means and standard deviations obtained for the study groups.

Groups	ΔE_{00}	Acceptable match*	TP_{00}	ΔTP_{00}	Acceptable match**
C	-	-	11.78 ^A (0.67)	-	-
G	3.44 ^A (0.64)	Yes	10.76 ^B (0.63)	1.02	Yes
SL	3.78 ^A (0.70)	Yes	10.69 ^B (0.96)	1.09	Yes

Different letters within a column indicate statistically significant differences among the study groups ($p < 0.05$, t-test for ΔE_{00} , and one-way ANOVA and Tukey's test for TP_{00}). ΔE_{ab} , color difference between G and SL groups. * Acceptable match if $\Delta E_{ab} \leq 1.2$.²⁰ ** Acceptable match if $\Delta TP_{00} > 0.6, \leq 2.6$.²⁰

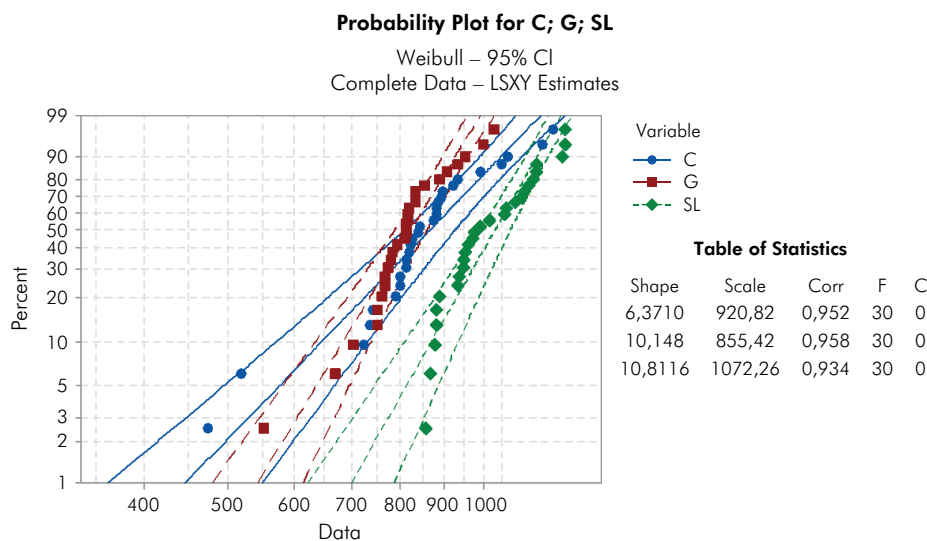


Figure 3. Weibull distribution graphs for groups C, G, and SL.

Borosilicate glass improved the flexural strength of 3Y-TZP by approximately 19%. Boron concentrations of around 3% (as utilized in this study) have been reported to enhance the elastic modulus and hardness of silicate glasses, thereby potentially increasing strength.²⁵ As highlighted by Campos et al.⁸, the high sintering temperature for silicate glass can facilitate the movement of zirconia grains and fill defects in the ceramic's microstructure. Additionally, boron has been reported in the literature as a component that decreases material viscosity, contributing to the low roughness values (Ra and Rz) observed for the SL group (Figure 1, Table 2).²⁶ Even with the extended firing, the commercial glaze resulted in flexural strength similar to that observed for the as-sintered control group, confirming the findings from previous studies (Table 2).¹¹

The Vickers indentation method was chosen for fracture toughness calculation because it could detect surface differences caused by thin layers of glaze or experimental glass. Fracture toughness significantly decreased when glaze and borosilicate were applied. This decrease was attributed to the load being applied on the glaze and borosilicate glass, which are weaker than zirconia. 3Y-TZP displays a toughness mechanism known as martensitic transformation.²⁷ When a crack develops in the material, the tetragonal grains transform into monoclinic, leading to an increase in volume by 3% to 5%. This growth prevents the crack from growing and, consequently, resists its propagation.^{27,28} As a result, the values of flexural strength and hardness are substantially increased compared to other ceramic materials (Table 2).²⁹ However, when a glaze layer is applied onto 3Y-TZP, the surface

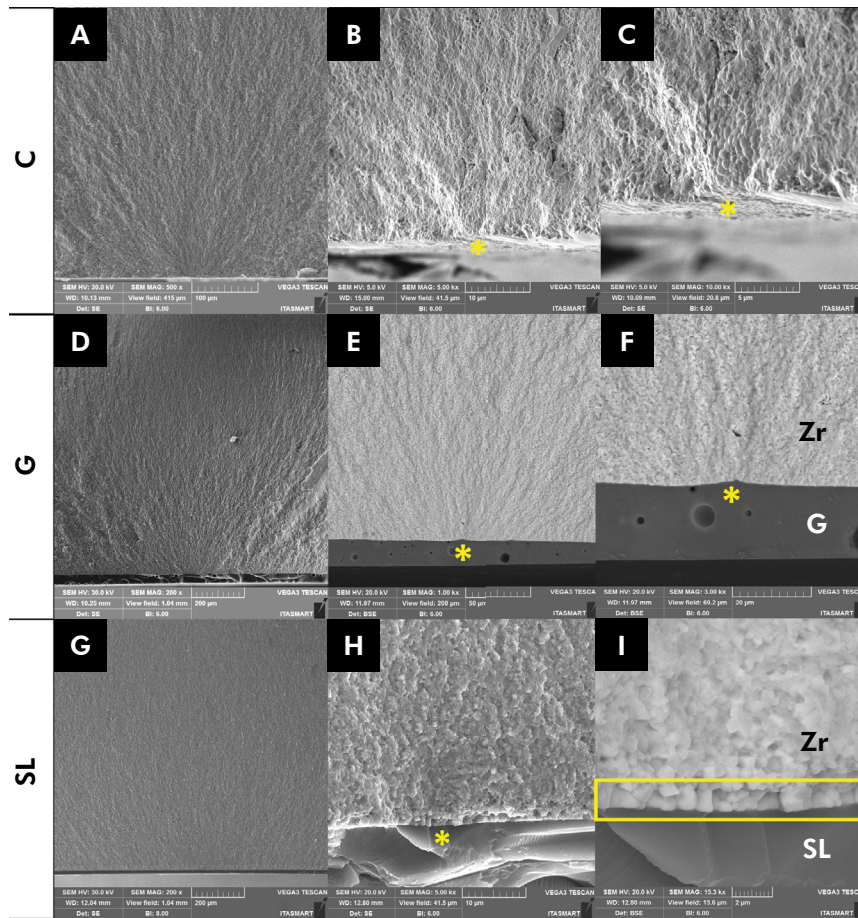


Figure 4. SEM images of the fractured surfaces according to the study groups. Group C (a, 500x; b, 5000x; and c, 10000x). Group G (d, 200x; e, 1000x; and f, 3000x). Group SL (g, 200x; h, 5000x, and i, 15000x). The origin of the fracture is indicated by a yellow asterisk. Monoclinic grains formed on the interface between borosilicate glass and zirconia are indicated by a yellow rectangle. Zr, zirconia; G, glaze; SL, borosilicate glass. All fractures originated on the tensile side of the specimens.

toughness drastically drops due to the lack of the phase transformation effect. On the other hand, borosilicate glass led to slightly higher toughness values than those of the commercial glaze (Table 2). These results might be related to the compressive stresses caused by the lower CTE of the experimental glass (approximately $3.5 \times 10^{-6} \text{ K}^{-1}$) compared to that of zirconia (approximately $10.8 \times 10^{-6} \text{ K}^{-1}$).

The borosilicate glass interacted with the first layer of grains due to its wettability, inducing the transformation of tetragonal grains into monoclinic grains (Figures 2 and 4). This transformation is associated with the XRD results, in that this analysis showed the formation of the monoclinic phase (Figure 2). The presence of monoclinic grains facilitates crack compression, consequently increasing biaxial flexural

strength, as observed in our results.¹⁸ This process is akin to hydrothermal degradation, where, at high temperatures, the glass (in a liquid state) acts similarly to water, penetrating the zirconia microstructure and inducing the tetragonal-to-monoclinic phase transformation (Figure 4, g and h).¹³ This phenomenon was also observed in the study by Campos et al.⁸ The authors developed an in-house glass with a composition similar to that of the present study, and compressive stress formation was observed in the group with glass due to the transformation of tetragonal to monoclinic phase zirconia. The XRD pattern of the borosilicate glass group also revealed the presence of the cubic phase. Zirconias with a higher cubic content typically exhibit lower strength.^{22,30} However, the low cubic content triggered by the

application of borosilicate glass was not sufficient to diminish the flexural strength (Figure 2).

The Weibull graph indicated no statistical difference between the G and SL groups (Figure 3). Borosilicate glass and glaze exhibited a homogeneous microstructural behavior, minimizing surface defects (Figure 4, e through h), resulting in similar Weibull modulus variability, in line with the findings by Campos et al.¹⁹

The fractographic analysis revealed that the failure origin was in the zirconia surface for all groups (Figure 4). Backscattered images were captured to identify the materials. Commercial glaze and borosilicate glass are distinguishable since their atomic weight is lower than that of zirconia.¹³ Since zirconia is denser, it is represented by a lighter color, whereas both glasses are displayed in darker colors. In a cross-section view, the glaze group exhibited bubbles within the glaze layer (Figure 4, e and f), which were not observed in the SL group. For the borosilicate glass group, the fracture occurred due to detachment of monoclinic grains located at the interface between zirconia and borosilicate glass, as shown in Figure 4, h and i.

Cubic grains enable a more uniform emission of incident light due to their isotropic characteristics.³¹ The way light interacts with cubic grains results in higher translucency. Even with the detection of the cubic phase in the SL group, it was not sufficient to affect translucency, since TP_{00} values were similar when borosilicate glass or glaze were applied. Both SL and G led to significantly lower translucency than the control, which can be attributed to the increase in thickness when the glassy layer was applied. Despite the statistical difference, the TP_{00} differences between SL or G and the control fall

within the acceptable match category defined by Paravina et al.²⁰ ($\Delta TP_{00} > 0.6, \leq 2.6$; Table 3).

On the other hand, the color differences observed in SL and G were statistically similar, and the difference between them corresponded to an excellent match ($\Delta E_{ab} \leq 1.2$), as confirmed by Paravina et al.²⁰ (Table 3). Figure 1 shows how the glassy surface changed the final appearance of the material. Light scatters more at the 3Y-TZP grain boundaries than at the glass matrix. The change in light interaction when a glassy material is applied over zirconia results in higher luminosity and color alteration. However, the color difference caused by borosilicate glass was similar to that caused by the commercial glaze, indicating the feasibility of the experimental glass.

This is an inaugural investigation on an alternative glass for the finishing of monolithic 3Y-TZP restorations. Our findings indicate that the material tested is promising. Finishing treatments capable of enhancing the mechanical properties of the materials are considered advantageous. Nonetheless, further investigations into wear and fatigue, specifically involving crown-shaped specimens, are recommended to validate the viability of utilizing borosilicate glass.

Conclusion

Borosilicate glass imparted a smoother surface to 3Y-TZP specimens compared to commercial glaze, and application of this experimental glass resulted in an enhancement of specimen biaxial flexural strength. Moreover, the influence of borosilicate glass on the optical properties of 3Y-TZP was similar to that of a commercial glaze.

References

1. Selvaraj U, Koli DK, Jain V, Nanda A. Evaluation of the wear of glazed and polished zirconia crowns and the opposing natural teeth: A clinical pilot study. *J Prosthet Dent.* 2021 Jul;126(1):52-7. <https://doi.org/10.1016/j.prosdent.2020.04.007>
2. Zucuni CP, Pereira GKR, Dapieve KS, Rippe MP, Bottino MC, Valandro LF. Low-fusing porcelain glaze application does not damage the fatigue strength of Y-TZP. *J Mech Behav Biomed Mater.* 2019;(99):198-205. <https://doi.org/10.1016/j.jmbbm.2019.07.022>
3. Oblak C, Kocjan A, Jevnikar P, Kosmac T. The effect of mechanical fatigue and accelerated ageing on fracture resistance of glazed monolithic zirconia dental bridges. *J Eur Ceram Soc.* 2017;37(14):4415-22. <https://doi.org/10.1016/j.jeurceramsoc.2017.04.048>

4. Manziuc MM, Gasparik C, Burde AV, Colosi HA, Negucioiu M, Dudea D. Effect of glazing on translucency, color, and surface roughness of monolithic zirconia materials. *J Esthet Restor Dent*. 2019 Sep;31(5):478-85. <https://doi.org/10.1111/jerd.12493>
5. Zucuni CP, Pereira GK, Valandro LF. Grinding, polishing and glazing of the occlusal surface do not affect the load-bearing capacity under fatigue and survival rates of bonded monolithic fully-stabilized zirconia simplified restorations. *J Mech Behav Biomed Mater*. 2020 Mar;103(103):103528. <https://doi.org/10.1016/j.jmbbm.2019.103528>
6. Janyavula S, Lawson N, Cakir D, Beck P, Ramp LC, Burgess JO. The wear of polished and glazed zirconia against enamel. *J Prosthet Dent*. 2013 Jan;109(1):22-9. [https://doi.org/10.1016/S0022-3913\(13\)60005-0](https://doi.org/10.1016/S0022-3913(13)60005-0)
7. Passos SP, Torrealba Y, Major P, Linke B, Flores-Mir C, Nychka JA. In vitro wear behavior of zirconia opposing enamel: a systematic review. *J Prosthodont*. 2014 Dec;23(8):593-601. <https://doi.org/10.1111/jopr.12167>
8. Campos TM, Melo Marinho RM, Ribeiro AD, Montanheiro TL, Silva AC, Thim GP. Microstructure and mechanical properties of fully sintered zirconia glazed with an experimental glass. *J Mech Behav Biomed Mater*. 2021;104093(113):104093. <https://doi.org/10.1016/j.jmbbm.2020.104093>
9. Aurélio IL, Fraga S, Dorneles LS, Bottino MA, May LG. Extended glaze firing improves flexural strength of a glass ceramic. *Dent Mater*. 2015 Dec;31(12):e316-24. <https://doi.org/10.1016/j.dental.2015.10.012>
10. Aurélio IL, Dorneles LS, May LG. Extended glaze firing on ceramics for hard machining: crack healing, residual stresses, optical and microstructural aspects. *Dent Mater*. 2017 Feb;33(2):226-40. <https://doi.org/10.1016/j.dental.2016.12.002>
11. Rodrigues CD, Aurélio IL, Fraga S, Kaizer MD, Zhang Y, May LG. Extended glaze firings for porcelain-veneered zirconia: effects on the mechanical and optical behavior. *Dent Mater*. 2021 Jul;37(7):1096-106. <https://doi.org/10.1016/j.dental.2021.03.009>
12. Callister WD, Rethwisch DG. *Materials science and engineering an introduction*. 8th ed. John Wiley & Sons; 2013.
13. Silva AC, Ribeiro AD, Alves LM, Ribeiro FC, Campos TB, Marinho RM. Zirconia gradation and thermal expansion compatibility between infiltration glass and antimicrobial glass. *Ceram Int*. 2022;48(14):19746-56. <https://doi.org/10.1016/j.ceramint.2022.03.242>
14. Brauer DS. Bioactive glasses: structure and properties. *Angew Chem Int Ed Engl*. 2015 Mar;54(14):4160-81. <https://doi.org/10.1002/anie.201405310>
15. Howes AP, Vedishcheva NM, Samoson A, Hanna JV, Smith ME, Holland D, et al. Boron environments in Pyrex® glass: a high resolution, Double-Rotation NMR and thermodynamic modelling study. *Phys Chem Chem Phys*. 2011 Jul;13(25):11919-28. <https://doi.org/10.1039/c1cp20771g>
16. Tien CL, Lee CC, Chuang KP, Jaing CC. Simultaneous determination of the thermal expansion coefficient and the elastic modulus of Ta₂O₅ thin film using phase shifting interferometry. *J Mod Opt*. 2000;47(10):1681-91. <https://doi.org/10.1080/09500340008231417>
17. Hayashi H, Saitou T, Maruyama N, Inaba H, Kawamura K, Mori M. Thermal expansion coefficient of yttria stabilized zirconia for various yttria contents. *Solid State Ion*. 2005;176(5-6):613-9. <https://doi.org/10.1016/j.ssi.2004.08.021>
18. Zanotto ED, Migliore AR Jr. Propriedades mecânicas de materiais cerâmicos: uma introdução. *Cerâmica*. 1991;(37):7-16.
19. Campos TM, Ramos NC, Machado JP, Bottino MA, Souza RO, Melo RM. A new silica-infiltrated Y-TZP obtained by the sol-gel method. *J Dent*. 2016 May;48(48):55-61. <https://doi.org/10.1016/j.jdent.2016.03.004>
20. Paravina RD, Pérez MM, Ghinea R. Acceptability and perceptibility thresholds in dentistry: A comprehensive review of clinical and research applications. *J Esthet Restor Dent*. 2019 Mar;31(2):103-12. <https://doi.org/10.1111/jerd.12465>
21. Zhang Y, Lawn BR. Novel Zirconia Materials in Dentistry. *J Dent Res*. 2018 Feb;97(2):140-7. <https://doi.org/10.1177/0022034517737483>
22. Rodrigues CS, Dhital S, Kim J, May LG, Wolff MS, Zhang Y. Residual stresses explaining clinical fractures of bilayer zirconia and lithium disilicate crowns: A VFEM study. *Dent Mater*. 2021 Nov;37(11):1655-66. <https://doi.org/10.1016/j.dental.2021.08.019>
23. López-Esteban S, Bartolomé JF, Dí Az LA, Esteban-Tejeda L, Prado C, López-Piriz R, et al. Mechanical performance of a biocompatible biocide soda-lime glass-ceramic. *J Mech Behav Biomed Mater*. 2014 Jun;34(34):302-12. <https://doi.org/10.1016/j.jmbbm.2014.02.019>
24. Deilmann L, Winter O, Cerrutti B, Bradtmüller H, Herzig C, Limbeck A, et al. Effect of boron incorporation on the bioactivity, structure, and mechanical properties of ordered mesoporous bioactive glasses. *J Mater Chem B*. 2020 Feb;8(7):1456-65. <https://doi.org/10.1039/C9TB01805K>
25. Nishimura S, Matsumoto S, Terashima K. Variation of silicon melt viscosity with boron addition. *J Cryst Growth*. 2002;237-239(237):1667-70. [https://doi.org/10.1016/S0022-0248\(01\)02317-X](https://doi.org/10.1016/S0022-0248(01)02317-X)
26. Chevalier J, Gremillard L, Virkar AV, Clarke DR. The tetragonal-monoclinic transformation in zirconia: lessons learned and future trends. *J Am Ceram Soc*. 2009;92(9):1901-20. <https://doi.org/10.1111/j.1551-2916.2009.03278.x>
27. Chevalier J, Olagnon C, Fantozzi G. Subcritical crack propagation in 3y-tzp ceramics: static and cyclic fatigue. *J Am Ceram Soc*. 1999;82(11):3129-38. <https://doi.org/10.1111/j.1151-2916.1999.tb02213.x>
28. Larsson C, Holm L, Lövgren N, Kokubo Y, Steyern PV. Fracture strength of four-unit Y-TZP FPD cores designed with varying connector diameter. An in-vitro study. *J Oral Rehabil*. 2007 Sep;34(9):702-9. <https://doi.org/10.1111/j.1365-2842.2007.01770.x>

29. Kwon SJ, Lawson NC, McLaren EE, Nejat AH, Burgess JO. Comparison of the mechanical properties of translucent zirconia and lithium disilicate. *J Prosthet Dent.* 2018 Jul;120(1):132-7. <https://doi.org/10.1016/j.prosdent.2017.08.004>
30. Stawarczyk B, Keul C, Eichberger M, Figge D, Edelhoff D, Lümke N. Three generations of zirconia: from veneered to monolithic. Part I. *Quintessence Int.* 2017;48(5):369-80. <https://doi.org/10.3290/j.qi.a38057>
31. Alves LM, Rodrigues CS, Vardhaman S, Saunders C, Schneider JM, Lawn BR, et al. Exploring Ductility in Dental Ceramics. *J Dent Res.* 2022 Nov;101(12):1467-73. <https://doi.org/10.1177/00220345221100409>